

**Supplemental Table S1.** Clinical Characteristics of the Study Populations. Values are presented as means  $\pm$  standard deviation (STD) in LTRC Yale Cohort (A), Pittsburgh Cohort (B) and Korean Asan cohort (C), respectively.

# The Global Initiative for Chronic Obstructive Lung Disease (GOLD) stage range from stage 1 (GOLD 1) COPD, indicating mild disease, to stage IV (GOLD 4) COPD, indicating very severe disease. § FEV<sub>1</sub>(%), pre-BD denotes prebronchodilator FEV<sub>1</sub> (% of predicted value). FEV<sub>1</sub>(%), post-BD denotes postbronchodilator FEV<sub>1</sub> (% of predicted value). D<sub>LCO</sub> denotes diffusing capacity. The BODE index stands for body mass index (BMI), obstruction, dyspnea and exercise capacity. The SGRQ score denotes Saint George Respiratory Questionnaires score. The BORG scale at termination is the extent of perceived patient exertion that can be estimated by the Borg scale at the termination of exercise.

(A) LTRC Cohort

Characteristic <sup>§</sup>	Control	COPD <sup>#</sup>			
		GOLD 1	GOLD 2	GOLD 3	GOLD 4
Number	7	6	10	10	10
age (yr)	57.7 $\pm$ 10.7	73.7 $\pm$ 6.9	66.3 $\pm$ 9.7	64.2 $\pm$ 6.9	54.0 $\pm$ 7.2
Gender (Male : Female)	(2 : 5)	(5 : 1)	(10 : 0)	(7 : 3)	(6 : 4)
Smokers ( Non-smokers)	3 (4)	6	10	10	10
Smoking history – pack-yr	15.4 $\pm$ 19.5	36.5 $\pm$ 10.8	54.1 $\pm$ 24.6	62.0 $\pm$ 25.7	51.8 $\pm$ 38.2
FEV <sub>1</sub> (%), Pre-BD	93.0 $\pm$ 12.1	82.7 $\pm$ 10.3	61.6 $\pm$ 6.9	32.2 $\pm$ 4.2	21.5 $\pm$ 7.7
FEV <sub>1</sub> (%), Post BD	98.2 $\pm$ 12.4	89.2 $\pm$ 6.9	67.7 $\pm$ 5.6	34.2 $\pm$ 3.3	19.8 $\pm$ 2.8
D <sub>LCO</sub>	96.4 $\pm$ 26.6	80.4 $\pm$ 16.9	51.75 $\pm$ 24.6	31.3 $\pm$ 6.3	39.2 $\pm$ 16.6
6 minute Walking-Distance	413.5 $\pm$ 43.8	321. $\pm$ , 35.6	318.5 $\pm$ 168.9	237.2 $\pm$ 88.9	270.5 $\pm$ 69.6
BODE Index	0.1 $\pm$ 0.4	1.1 $\pm$ 1.1	2.9 $\pm$ 2.6	6.8 $\pm$ 1.6	6.8 $\pm$ 1.1
SGRQ Score	5.3 $\pm$ 9.8	18.1 $\pm$ 20.6	36.9 $\pm$ 27.7	67.0 $\pm$ 10.9	59.2 $\pm$ 15.1
BORG Scale at Termination	0.8 $\pm$ 0.3	1.0 $\pm$ 1.4	3.3 $\pm$ 1.4	4.3 $\pm$ 1.9	4.9 $\pm$ 2.6
NLRX1 mRNA (standardized)	1.22 $\pm$ 0.73	1.35 $\pm$ 0.39	1.22 $\pm$ 0.63	0.78 $\pm$ 0.29	0.73 $\pm$ 0.28

### (B) Pittsburgh Cohort

<b>Characteristic</b>	<b>Control (n=63)</b>	<b>&lt; 1% emphysema (n=20)</b>	<b>1-10% emphysema (n=51)</b>	<b>&gt; 40% emphysema (n=26)</b>
Age	65.8±10.3	67.9±8.4	68.4±8.4	56.2±7.2
Female Gender	27 (43%)	8 (40%)	17 (33%)	16 (62%)
Race	2 African-American 58 Caucasian 3 Other	20 Caucasian	1 African-American 50 Caucasian	26 Caucasian
Pack-Years	26.3±34.3	56.1±31.2	65.1±40.0	50.8±25.6
FEV1 (% predicted)	97.4±9.2	63.5±12.0	60.3±13.9	24.2±8.2
FVC (% predicted)	93.3±11.8	74.9±12.7	83.4±15.7	56.0±18.7
DLCO (% predicted)	81.9±16.3	70.4±21.8	62.4±16.1	31.5±8.5
HU < -950 (%)	0.7±1.1	0.4±0.3	4.2±2.5	48.7±6.9

### (C) Asan Cohort

<b>Characteristic</b>	<b>Control</b>	<b>GOLD 1</b>	<b>GOLD 2</b>	<b>GOLD 3</b>
Number (M : F)	94 (94 : 0)	45 (45 : 0)	53 (53 : 0)	1 (1 : 0)
age (mean, STD)	60.6 ± 9.4	68.3 ± 6.1	66.9 ± 6.5	61
Smoker ( NS : CS)	(94 : 0)	(45 : 0)	(53 : 0)	(1 : 0)
PKYrs (mean, STD)	34.8 ± 17.1	49.5 ± 19.4	46.3 ± 24.1	40
FEV1 (%), Pre-BD (mean, STD)	91.0 ± 12.4	83.7 ± 8.3	63.5 ± 7.6	28
FEV1 (%), Post BP (mean, STD)	94.3 ± 12.8	89.2 ± 6.8	68.4 ± 6.7	34
D <sub>LCO</sub> (mean, STD)	92.9 ± 12.9	78.3 ± 13.9	76.1 ± 14.6	86
NLRX1 transcriptome (mean, STD)	2.22 ± 1.49	1.69 ± 1.34	1.39 ± 0.87	1.06

## Supplemental Figures

**Figure S1.** (A) The levels of NLRX1 protein in mitochondria-enriched tissue fractions (MF) from controls (0) and GOLD 1, 2, 3, and 4 individuals were evaluated by western blot analysis. NLRX1 is compared to the levels of the voltage dependent anion channel (VDAC) (A) and in (B), were evaluated by densitometry (\*\*  $p < 0.01$ , Mann-Whitney U test).

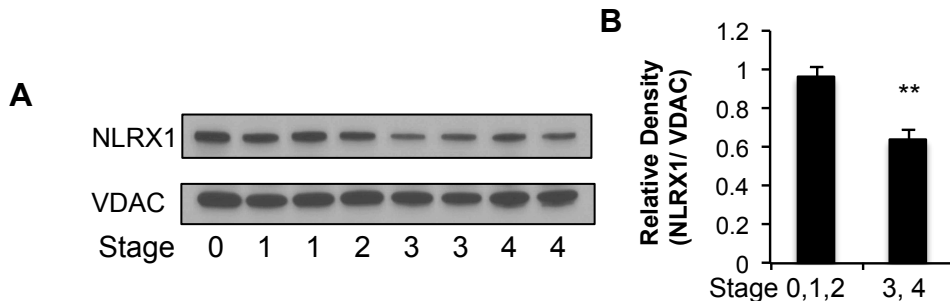


**Figure S2.** Statistical evaluations of subgroups Korean Asan cohort. Because only one patient was in GOLD3, this subgroup was not used in these comparisons. (\* For the overall comparison between all subgroups, please see the figure 1(h)). ANOVA evaluations were employed.

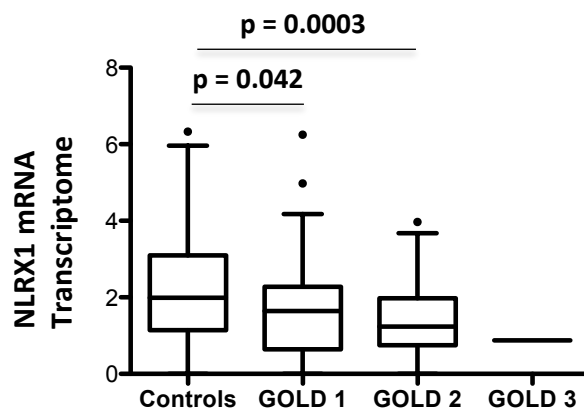


**Figure S3.** The correlations between the levels of (A) NLRX1 mRNA and pre-bronchodilator  $FEV_1$  (% of predicted value) and (B) NLRX1 mRNA and post-bronchodilator  $FEV_1$  (% of predicted value), respectively, in the Korean Asan cohort. Pearson correlation analysis was employed.

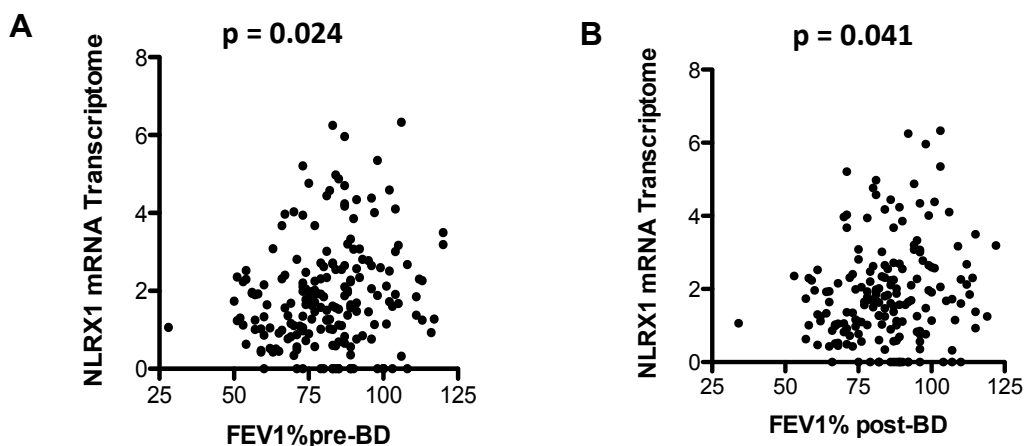


Figure S4. Comparisons of the levels of NLRX1 mRNA and smoking status in the Korean Asan cohort. A two-tailed t-test was applied in this evaluation.

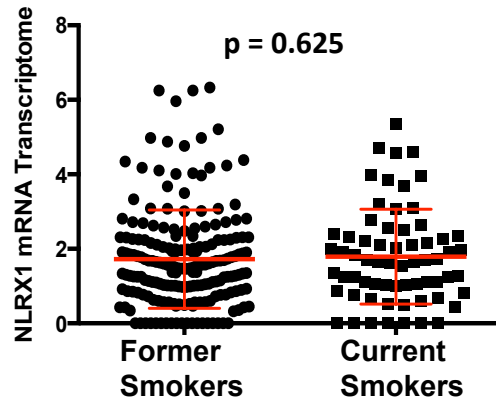


Figure S5. The levels of (A) MAVS mRNA and (B) protein in LTRC samples were plotted in controls (0) and in patients with COPD of varying severity (GOLD 1, 2, 3, and 4). N.S., not significant (Kruskal-Wallis test).

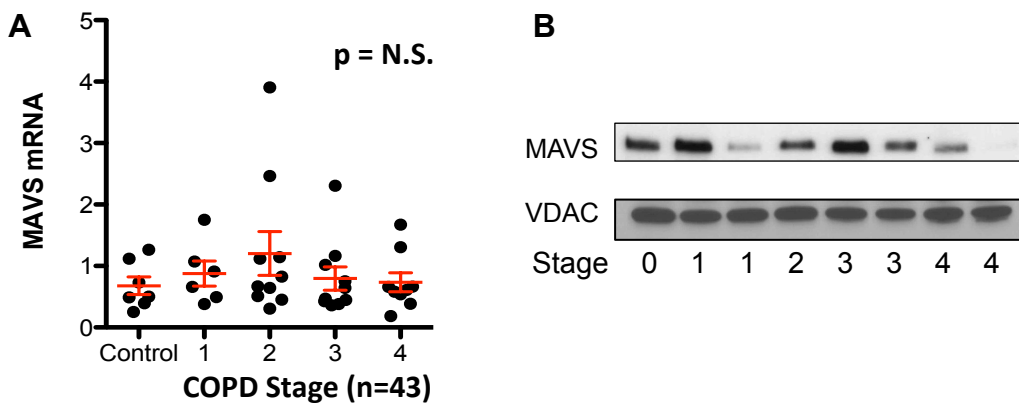
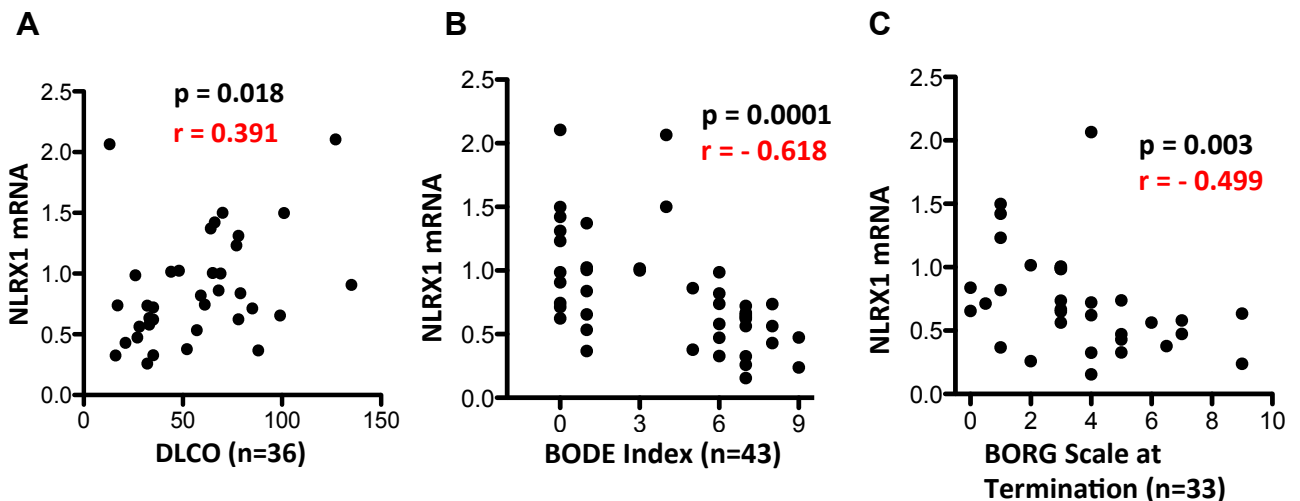
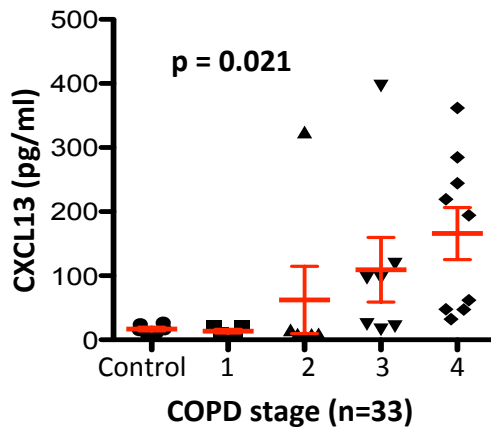


Figure S6. The correlations between the levels of NLRX1 mRNA and (A) diffusing capacity (DLCO), (B) BODE index, and (C) BORG scale, respectively, in the LTRC cohort. Pearson correlations were used in these evaluations.



**Figure S7.** Comparisons of the levels of CXCL13 protein in LTRC samples in controls (0) and in patients with COPD of varying severity (GOLD 1, 2, 3, and 4) (Kruskal-Wallis test).



**Figure S8.** Comparisons of the correlations between the levels of CXCL13 protein and (A) post-bronchodilator FEV<sub>1</sub>(% of predicted value), (B) NLRX1 mRNA, (C) BODE index, and (d) SGRQ score, respectively, in LTRC cohort (Pearson correlation analysis).

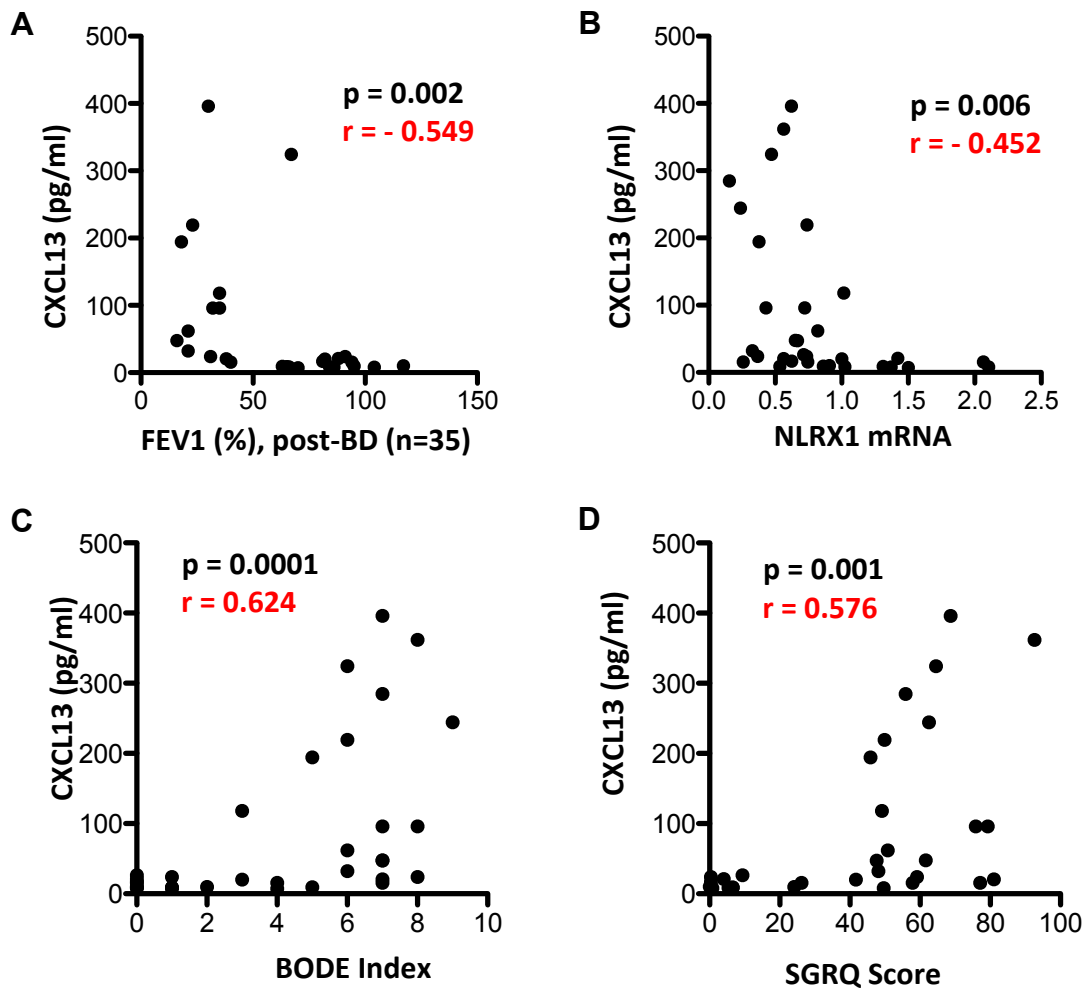


**Figure S9.** Characterization of the effects of CS on NLRX1 protein. On the left, Western blotting is used to compare NLRX1 and VDAC. The bar graph to the right illustrates the densitometric evaluations of the levels of NLRX1 and VDAC. Mitochondria-enriched fractions (MF) and cytosol-enriched fractions (CF) in four similar experiments were used (\*  $p < 0.05$ , Mann-Whitney U test).

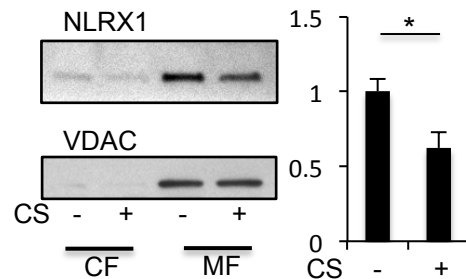


**Figure S10.** Immunohistochemical analysis of NLRX1 in murine lungs. Representative pictures of non-smoking controls from (A) wild type mice and (B) NLRX1<sup>-/-</sup> mutant mice are presented. Red-colored staining in wild type mice, which are not observed in NLRX1<sup>-/-</sup> mutant mice, are most prominent in alveolar macrophages (magnification X20).

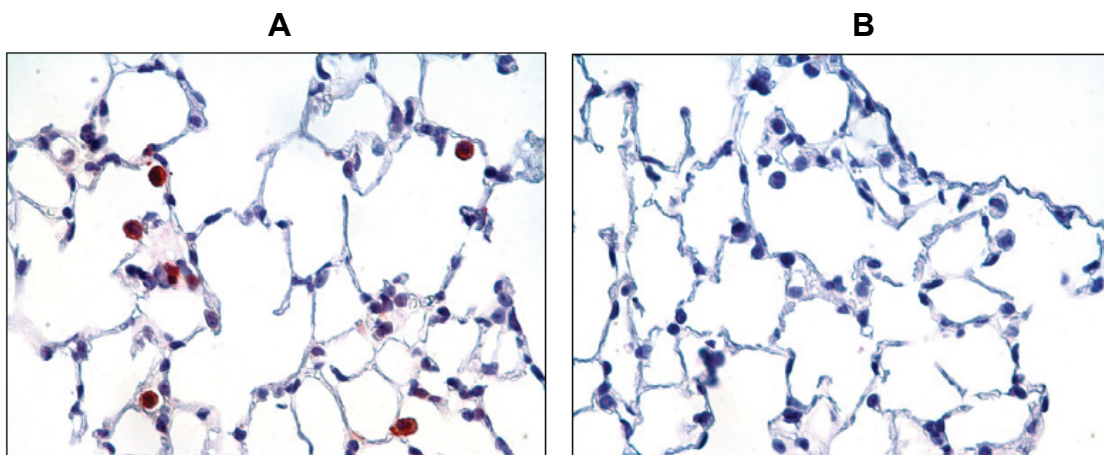


**Figure S11.** Representative Immunohistochemical evaluations of NLRX1 in normal human lung tissues at (A) low magnification (X4) and (B) higher magnification (X40). Red-colored staining was most prominently observed in alveolar macrophages.

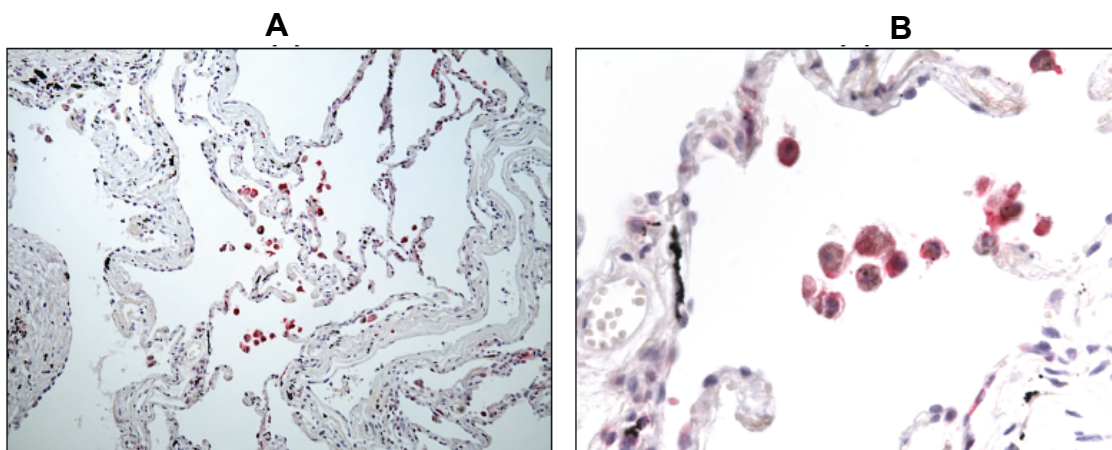


**Figure S12.** Densitometric evaluations of the Western blot presented on figure 2(c). (A) NLRX1 expression and (B) MAVS expression. (\*\* p < 0.01, Mann-Whitney U test).

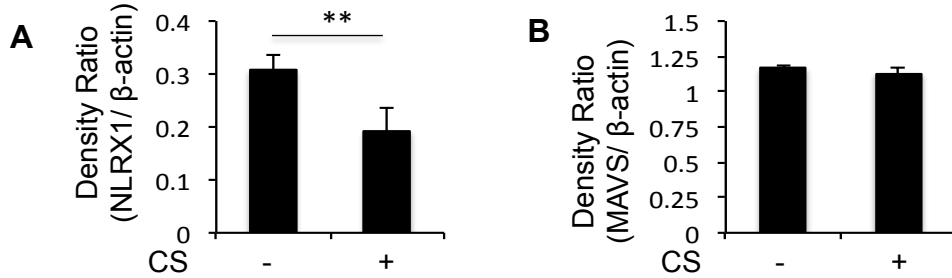


**Figure S13.** The suppression of NLRX1 mRNA accumulation in 3-month cigarette smoke-exposed lungs (CS +) and its recovery 3 months after the cessation of CS exposure (#) (\*\* p < 0.01, Kruskal-Wallis test).

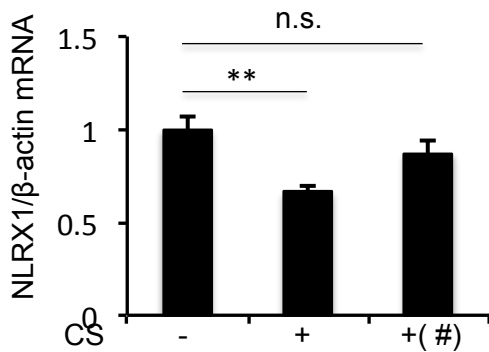


**Figure S14.** Representative histology after 3 months of CS exposure in the lungs from WT (NLRX1+/+) and NLRX1 null (-/-) mice. Size bar on the lower right corner of each panel represents 400μm.

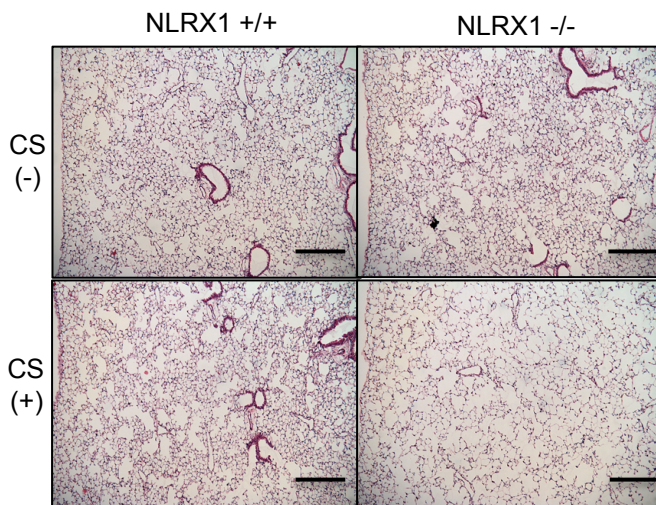


**Figure S15.** The enhancement of (A) MMP-12 mRNA expression, (B) IFN- $\alpha$ 4 mRNA expression, (C) epithelial DNA injury/cell death responses and (D) iL-1 $\beta$  production after 3-month cigarette smoke-exposure (CS +) in the lungs from NLRX1 deficient (NLRX1 $^{-/-}$ ) mice compared to those from WT controls (NLRX1 $^{+/+}$ ) ( \*\*  $p < 0.01$ , two-way ANOVA test).

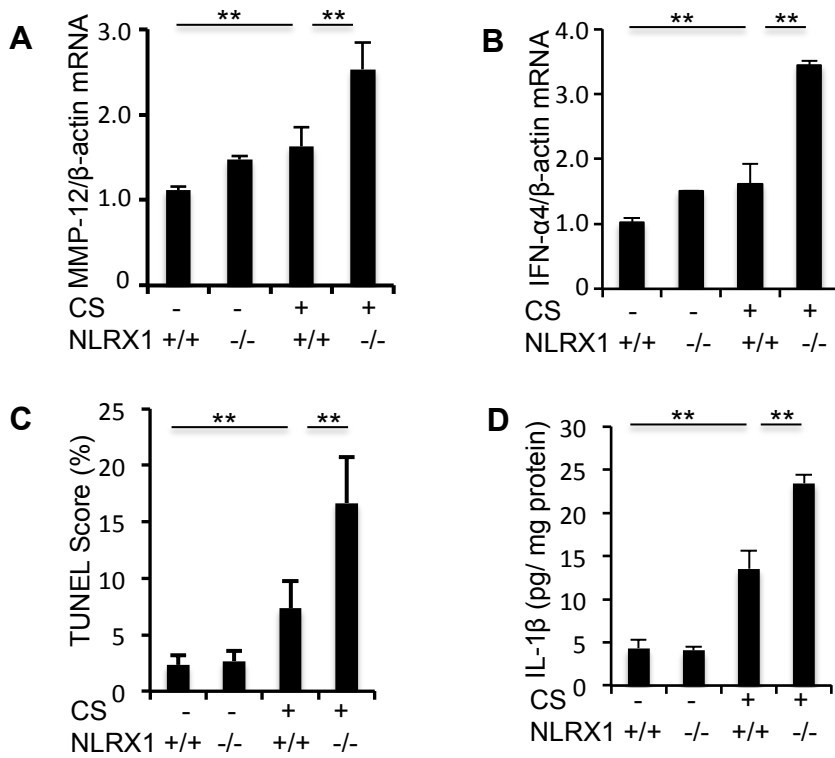


**Figure S16.** The enhancement of CXCL13 mRNA expression after 3-month cigarette smoke-exposure (CS +) in the lungs from NLRX1 deficient (NLRX1 $^{-/-}$ ) mice compared to those from WT controls (NLRX1 $^{+/+}$ ) (\*  $p < 0.05$ , \*\*  $p < 0.01$ , two-way ANOVA test).

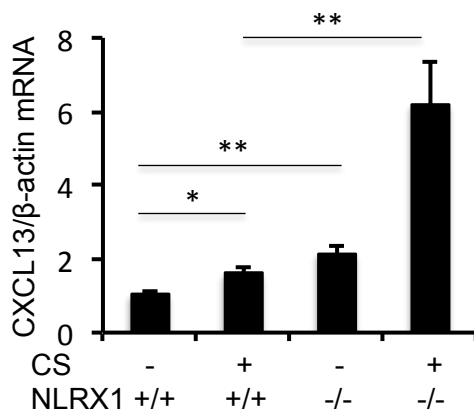


**Figure S17.** The effects of NLRX1 supplementation on CS-induced *in vivo* responses; (A) emphysematous alveolar destruction after 6-month-CS-exposure, (B) morphometric evaluation of alveolar size (\*  $p < 0.05$ , \*\*  $p < 0.01$ , Two-way ANOVA test; size bar = 400 $\mu$ m).

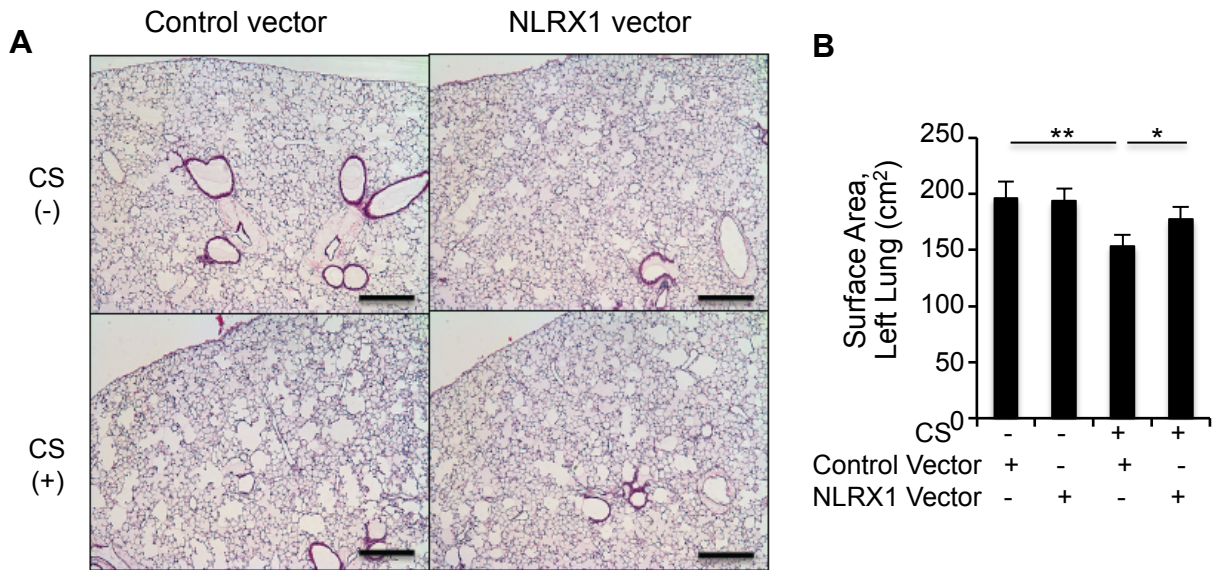


**Figure S18.** Representative histologies after 6 months of CS exposure in the lungs from WT (MAVS<sup>+/+</sup>) and MAVS null (-/-) mice.

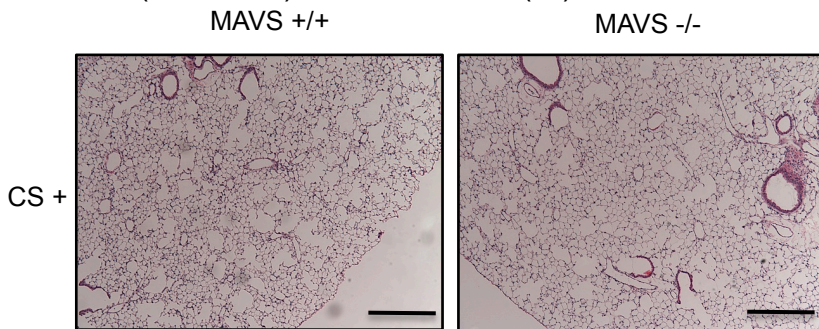


**Figure S19.** Comparisons of the levels of (A) MMP-12 mRNA, (B) interferon (IFN)- $\alpha$ 4 mRNA, (C) NLRX1 mRNA and (D) TUNEL Score (%) after 6 months of CS exposure in the lungs from WT (MAVS<sup>+/+</sup>) and MAVS null (-/-) mice (\* $p < 0.05$ , \*\*  $p < 0.01$ , two-way ANOVA test).

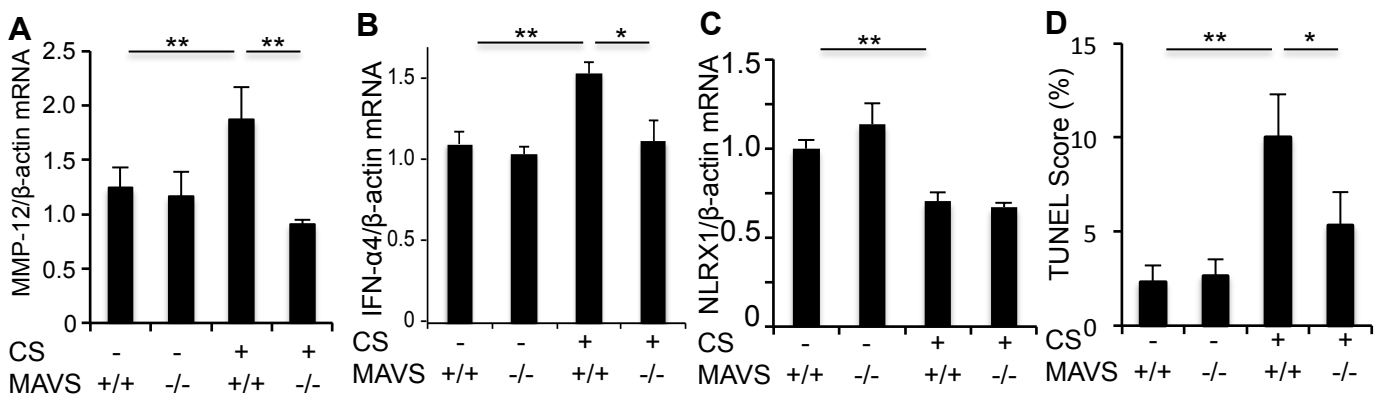


**Figure S20.** Representative histologies and measurements of alveolar surface area after 3-month-CS-exposure in wild type (WT) controls, NLRX1<sup>-/-</sup> and NLRX1<sup>-/-</sup>/MAVS<sup>-/-</sup> mice (\*\* p < 0.01, two-way ANOVA test; size bar = 400µm).

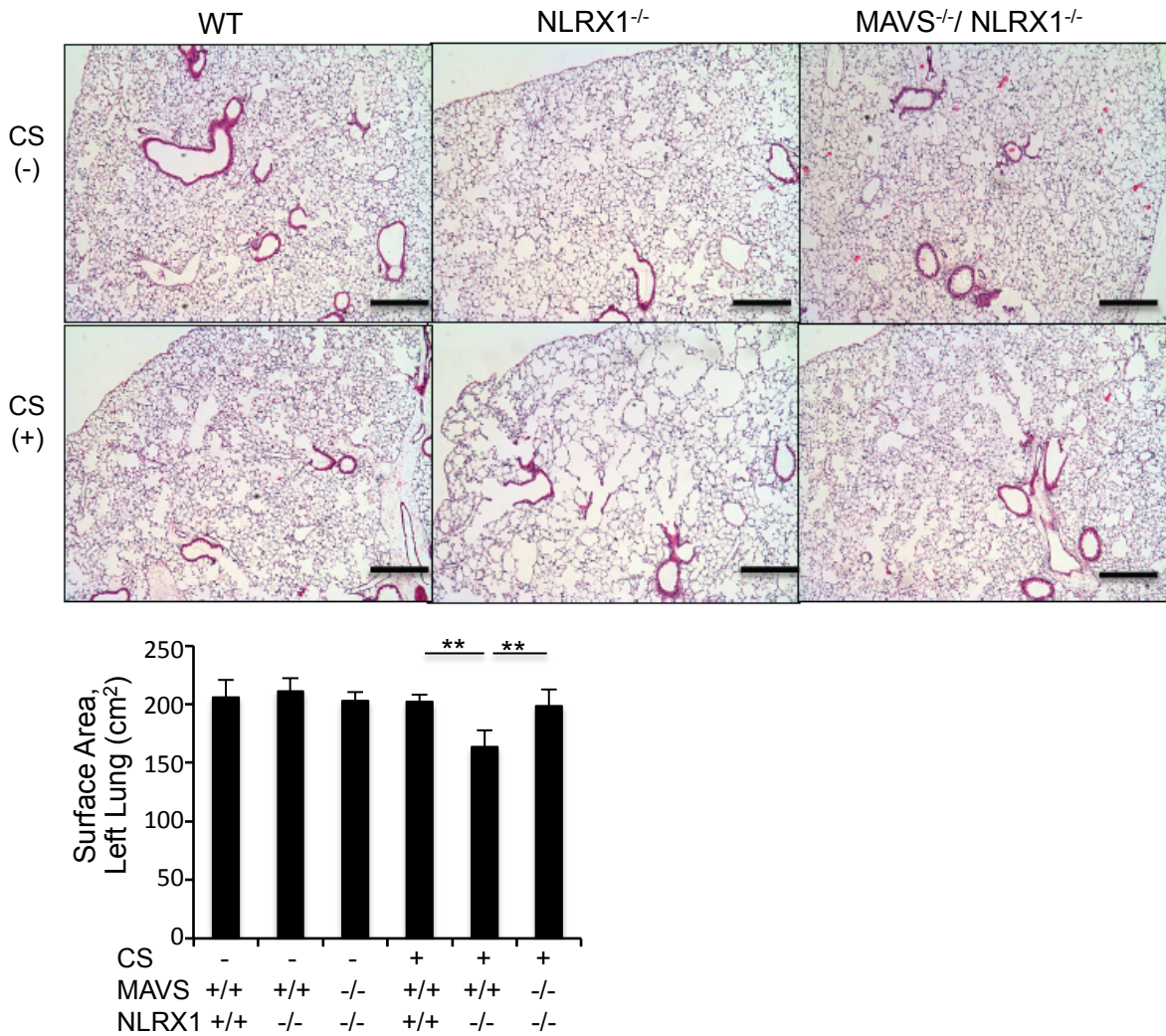
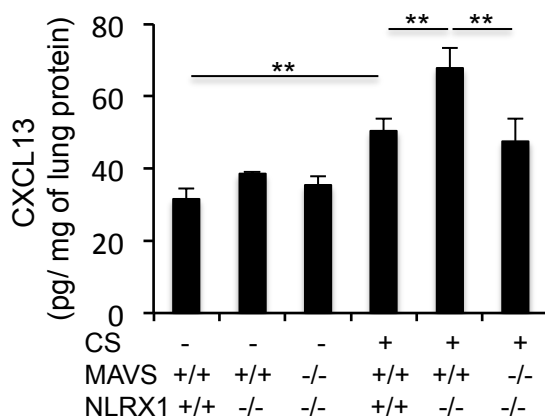


**Figure S21.** The enhancement of CXCL13 after 3-months of cigarette smoke-exposure (CS +) in the lungs from NLRX1 deficient (NLRX1<sup>-/-</sup>) mice compared to WT controls (NLRX1<sup>+/+</sup>) (\* p < 0.05, \*\* p < 0.01, two-way ANOVA test).



## On-Line Supplemental Methods

### Study Populations

Three cohorts were used in these studies. In the Yale cohort, fresh frozen lung tissues from 7 controls and 36 patients with COPD were obtained from the Lung Tissue Research Consortium (LTRC) (1), a nationwide resource program from the National Heart, Lung, and Blood Institute (NHLBI) that provides human lung tissues with highly qualified and extensive phenotype data. For the Pittsburgh cohort, lung tissues were obtained as previously described (2). Briefly, controls (n=63) were defined as the subjects who have no evidence of chronic lung disease as well as normal pulmonary function tests including lung volumes. The subjects with COPD had varying levels of emphysema which were measured by quantitative CT using HU < -950 as a cutoff. The subjects with COPD were further stratified by the amount of quantitative emphysema with the three categories including <1%, which denotes less than 1% emphysema (n=22); 1-10%, which denotes a low level of emphysema between 1 and 10 percent (n=45); and the most severe cases, with more than 40% emphysema (n=27). The characteristics of these patients can be seen in Table 1b. For the Asan cohort, subjects were patients who required resection for lung cancer and who were registered in the Asan Biobank. Inclusion criteria were a FEV1/FVC ratio of less than 0.7 for the COPD group, and normal spirometry for the control group. This study was approved by the institutional review board of Asan Medical Center (#2011-0711) and written informed consent was obtained from all patients.

### Mouse Models

All in vivo experiments in animals were approved by the Yale Animal Care and Use Committee (YACUC). The generation and basic characterization of MAVS null mutant ( $^{-/-}$ ) and

NLRX1<sup>-/-</sup> mice have been described previously (3, 4). MAVS<sup>-/-</sup> mice were gifts from Dr. Zhijian J Chen (Department of Molecular Biology, University of Texas Southwestern Medical Center, Dallas, Texas, 75390). The CS-induced murine emphysema model that was employed has been described previously (5, 6).

#### RNA preparation and sequencing for human studies

For the Yale cohort, we extracted the mRNAs from fresh frozen lung tissues from the 7 controls and 36 patients with COPD in the NIH-sponsored Lung Tissue Research Consortium (LTRC) cohort. cDNA synthesis and real-time reverse-transcriptase-polymerase-chain-reaction (RT-PCR) assays were performed with whole RNA extracted from fresh frozen human lung tissues using Bio-Rad kits as per the manufacturer's instructions. The human NLRX1 primers from Primerbank (7) were utilized for the evaluation of the Yale cohort. For the Asan cohort, total RNA was isolated from apparently normal fresh frozen lung tissue that was remote from the lung cancer. RNA integrity was assessed using an Agilent Bioanalyzer and RNA purity was assessed using a NanoDrop spectrophotometer. One µg of total RNA was used to generate cDNA libraries using the TruSeq RNA library kit. The protocol consisted of poly A-selected RNA extraction, RNA fragmentation, reverse transcription using random hexamer primers, and 100 bp paired-end sequencing using the Illumina HiSeq 2000 system. The libraries were quantified using quantitative PCR according to the quantitative PCR Quantification Protocol Guide and qualified using an Agilent Technologies 2100 Bioanalyzer. For quality control, read quality was verified using FastQC and read alignment was verified using Picard. Differential gene expression (DEG) analysis was performed using TopHat and Cufflinks software (8). To estimate expression levels, the RNA-seq reads were mapped to the human genome using TopHat (version 1.4.1) (9), and quantified using Cufflinks software (2.0.0) (10). Cufflinks software was run with the UCSC hg19

human genome and transcriptome references. The numbers of isoform and gene transcripts were calculated and the relative abundance of transcripts was measured in fragments per kilobase of exon per million fragments mapped (FPKM) using Cufflinks software. Expression levels were extracted as a FPKM value for each gene of each sample using Cufflinks software. Genes with FPKM values of 0 across all samples were excluded. Filtered data were subject to upper quantile normalization. Statistical significance was determined using Student's *t*-test. The false discovery rate (FDR) was controlled by adjusting *p* values using the Benjamini-Hochberg algorithm.

### Laboratory Assessments

Separation of the cytosol- and mitochondria-enriched fractions was undertaken using Qproteome mitochondrial isolation kit (Qiagen) as per the manufacturer's instructions. Immunoblot analyses were undertaken using antibodies for NLRX1 (Proteintech, #17215-1-AP, Chicago, IL for Rabbit anti-human NLRX1; Imgenex, #IMG-6680A, Toronto, Canada for rabbit anti-mouse NLRX1), MAVS (Cell Signaling, #4983, for anti-human MAVS; Cell Signaling, #3993 for anti-mouse MAVS), caspase-1 (Cell Signaling, #2225), IL-1 $\beta$  (Santa Cruz, #SC-7884), IL-18 (Santa Cruz, #SC-7954) and  $\beta$ -actin (Santa Cruz, #SC-47778 HRP). Immunohistochemistry for NLRX1 was undertaken to localize the expression of NLRX1. For the evaluation of lung morphometry, subgroups of 5–7 mice were used for the evaluation of mean chord length and the surface area of the lungs following stereological analysis of the lungs according to the ATS/ERS guidelines (11, 12). Briefly, the left lung was inflated with 0.5% low temperature-melting agarose in 10% buffered formalin fixative at a constant pressure of 25cm as described previously (5, 13). After the fixation, lung volume ( $V_L$ ) of the left lung was determined by the water immersion method. The images were taken equally spaced and systematically placed meander-like over the whole surface of the lung sections. Pictures were quantitatively

analyzed by using a test system of points and lines superimposed over the digital images via the STEPanizer program (14). The intersecting points falling on alveolar space ( $P_a$ ) and alveolar ducts ( $P_d$ ) were counted separately among total points ( $P_{total}$ ). Point counts yielded relative volume densities and alveolar surface area ( $S_A$ ) was calculated by the following formula; (1) Airspace fraction ( $F_A$ ) =  $(P_a+P_d)/P_{total}$ ; (2) Airspace volume ( $V_A$ ) =  $F_A \times V_L$ ; (3)  $S_A = 4V_A/L_m$  (mean linear intercept). In addition, mean chord length of the air space was evaluated as described previously by our laboratory(5, 13). Lung tissue lysates were prepared and the levels of tissue CXCL13, IL-1 $\beta$  and IL-18 (R&D Systems) were determined using commercial ELISA kits as per the manufacturer's instructions. For the evaluation of apoptotic cell death/ DNA injury, end labeling of exposed 3'-OH ends of DNA fragments in paraffin embedded tissue was undertaken with the TUNEL *in situ* cell death detection kit AP (Roche Diagnostics) using the instructions provided by the manufacturer. To overexpress NLRX1 gene *in vivo*, we integrated the gene into lentiviral vector. The lentiviral vector backbones used in this study were purchased from System Biosciences Inc. (SBI, CA, USA, Catalog #CD511B-1). The NLRX1 cDNA clone was purchased from Origene (Origene, MD, USA, Catalog #MC204753). pPACKH1-XL HIV Lentivector Packaging Kit (SBI, CA, USA, Catalog #LV510A-1) and virus precipitation solution (SBI, CA, USA, Catalog #LV810A-1) were used to package the lentiviral vectors, according to the manufacturer's instructions. The lentiviral titer kit (SBI, CA, USA, Catalog #LV961A-1) was used to determine the amount of viral vectors according to the manufacturer's instructions. Intranasal administration of either the lenti-NLRX1, or lenti-control vectors was performed on 6-wk-old C57BL/6J male mice. The amount of  $1 \times 10^8$  TU of lenti-NLRX1 or lenti-control vectors per mouse was administered. CS exposure experiment was started from 2 weeks after intranasal treatment.

## Statistical Analysis

The statistics that were applied for the human studies were the nonparametric Kruskal-Wallis test (Fig. 1A), Mann-Whitney U test (Fig. 1B & C), Pearson correlation analysis (Fig. 1D & E), one-way ANOVA with Tukey's HSD test (Fig. 1F and Fig. 1H), and two-tailed unpaired t-test (Fig. 1G). For the comparison of two groups of the murine data, two-tailed Student's *t* test (Fig. 2A) or nonparametric Mann-Whitney U test (Fig. 2B & C) were applied as appropriate. For the comparison of multiple groups of the murine data, two-way ANOVA with Tukey's HSD test was applied. Statistical significance was defined at a level of  $p \leq 0.05$ . All analyses were completed with SPSS software, version 22.0.

## REFERENCES

1. LTRC. Lung Tissue Research Consortium. <http://www.nhlbi.nih.gov/resources/ltrc.htm>.
2. Shi, Y., Cao, J., Gao, J., Zheng, L., Goodwin, A., An, C.H., Patel, A., Lee, J.S., Duncan, S.R., Kaminski, N., et al. 2012. Retinoic acid-related orphan receptor-alpha is induced in the setting of DNA damage and promotes pulmonary emphysema. *Am J Respir Crit Care Med* 186:412-419.
3. Sun, Q., Sun, L., Liu, H.H., Chen, X., Seth, R.B., Forman, J., and Chen, Z.J. 2006. The specific and essential role of MAVS in antiviral innate immune responses. *Immunity* 24:633-642.
4. Allen, I.C., Moore, C.B., Schneider, M., Lei, Y., Davis, B.K., Scull, M.A., Gris, D., Roney, K.E., Zimmermann, A.G., Bowzard, J.B., et al. 2011. NLRX1 protein attenuates inflammatory responses to infection by interfering with the RIG-I-MAVS and TRAF6-NF-kappaB signaling pathways. *Immunity* 34:854-865.
5. Kang, M.J., Homer, R.J., Gallo, A., Lee, C.G., Crothers, K.A., Cho, S.J., Rochester, C., Cain, H., Chupp, G., Yoon, H.J., et al. 2007. IL-18 is induced and IL-18 receptor alpha

- plays a critical role in the pathogenesis of cigarette smoke-induced pulmonary emphysema and inflammation. *J Immunol* 178:1948-1959.
6. Hautamaki, R.D., Kobayashi, D.K., Senior, R.M., and Shapiro, S.D. 1997. Requirement for macrophage elastase for cigarette smoke-induced emphysema in mice. *Science* 277:2002-2004.
  7. PrimerBank. <http://pga.mgh.harvard.edu/primerbank/>.
  8. Trapnell, C., Roberts, A., Goff, L., Pertea, G., Kim, D., Kelley, D.R., Pimentel, H., Salzberg, S.L., Rinn, J.L., and Pachter, L. 2012. Differential gene and transcript expression analysis of RNA-seq experiments with TopHat and Cufflinks. *Nat Protoc* 7:562-578.
  9. Trapnell, C., Pachter, L., and Salzberg, S.L. 2009. TopHat: discovering splice junctions with RNA-Seq. *Bioinformatics* 25:1105-1111.
  10. Trapnell, C., Williams, B.A., Pertea, G., Mortazavi, A., Kwan, G., van Baren, M.J., Salzberg, S.L., Wold, B.J., and Pachter, L. 2010. Transcript assembly and quantification by RNA-Seq reveals unannotated transcripts and isoform switching during cell differentiation. *Nat Biotechnol* 28:511-515.
  11. Hsia, C.C., Hyde, D.M., Ochs, M., and Weibel, E.R. 2010. An official research policy statement of the American Thoracic Society/European Respiratory Society: standards for quantitative assessment of lung structure. *Am J Respir Crit Care Med* 181:394-418.
  12. Muhlfeld, C., and Ochs, M. 2013. Quantitative microscopy of the lung: a problem-based approach. Part 2: stereological parameters and study designs in various diseases of the respiratory tract. *Am J Physiol Lung Cell Mol Physiol* 305:L205-221.
  13. Kang, M.J., Lee, C.G., Lee, J.Y., Dela Cruz, C.S., Chen, Z.J., Enelow, R., and Elias, J.A. 2008. Cigarette smoke selectively enhances viral PAMP- and virus-induced pulmonary innate immune and remodeling responses in mice. *J Clin Invest* 118:2771-2784.
  14. Tschanz, S.A., Burri, P.H., and Weibel, E.R. 2011. A simple tool for stereological assessment of digital images: the STEPanizer. *J Microsc* 243:47-59.